Distribution functions in the interior of polymer chains

1980 J. Phys. A: Math. Gen. 13 3525

(http://iopscience.iop.org/0305-4470/13/11/023)

J. Phys. A: Math. Gen. **13** (1980) 3525–3541. Printed in Great Britain

Distribution functions in the interior of polymer chains

S Redner

Center for Polymer Studies and Department of Physics, Boston University, 111 Cummington Street, Boston, MA 02215, USA

Received 31 January 1980, in final form 14 April 1980

Abstract. For a polymer chain in a good solvent, we calculate the probability distribution functions between an endpoint and an interior point, and between two interior points, by using exact enumeration to study a lattice self-avoiding walk model. We find that these distribution functions are different from the usual distribution function between endpoints. At small distance scales, the probability of nearest-neighbour contacts between two interior points is smaller than the probability of contact between two endpoints. The contact probability is found to vary with N, the number of monomers between the contacts, as $N^{-(d+\theta_2)\nu}$ with $(d+\theta_2)\nu = +2{\cdot}16 \pm 0{\cdot}20$ on the FCC, and $(d+\theta_2)\nu = +2{\cdot}95 \pm 0{\cdot}20$ on the triangular lattice. From this we deduce that the exponent θ_2 describing the short-distance spatial decay of the corresponding distribution function is $\theta_2 = 0{\cdot}67 \pm 0{\cdot}34$ and $\theta_2 = 1{\cdot}93 \pm 0{\cdot}27$ on the FCC and triangular lattices respectively. For large distance scales, we present evidence that the distribution functions vary as $\exp(-(r/N^{\nu})^{\delta_1})$, where ν is the correlation length exponent, and where the exponent δ_1 describes the large-distance spatial decay. On the square lattice we estimate that $\delta_1 = 4{\cdot}5 \pm 0{\cdot}4$ for the endpoint–interior distribution, and $\delta_2 = 4{\cdot}6 \pm 0{\cdot}6$ for the interior–interior distribution (while $\delta_0 = 4{\cdot}0$ for the endpoint problem). On the simple cubic lattice, we estimate $\delta_1 = 2{\cdot}6 \pm 0{\cdot}06$ (while $\delta_0 = 2{\cdot}5$).

1. Introduction

Much of our current understanding of the configuration of linear polymer chains in a good solvent is based on the study of the probability distribution function $P_N(\boldsymbol{r})$ (see e.g. de Gennes 1979). This is defined as the probability that one end of a polymer chain consisting of N monomers is located at $\boldsymbol{r}$, given that the other end is at the origin. This function behaves as

$$P_N(\boldsymbol{r}) = N^{-d\nu} f(r/N^{\nu}) \tag{1}$$

where d is the spatial dimension, ν is the correlation length exponent, and the scaling function f varies as $f(z) \sim z^{\theta}$ for $z \ll 1$, and $f(z) \sim \exp(-z^{\delta})$ for $z \gg 1$ (see figure 1).

The nature of this distribution function has been extensively investigated. Generally, the self-avoiding walk (SAW) model on a lattice has been employed in order to simulate polymer chains in a good solvent. Fisher (1958) first suggested that unlike the *random* walk model, the distribution function for SAW's was non-Gaussian. This was subsequently confirmed qualitatively by a Monte Carlo investigation (Wall and Erpenbeck 1959), and by an exact enumeration study (Fisher and Hiley 1961). By deriving more extensive data, Domb *et al* (1965) were able to study quantitatively the large-distance tail of the distribution function. They found that the exponent $\delta = 4{\cdot}0$ on the square lattice, and that $\delta = 2{\cdot}5$ on the simple cubic lattice. Fisher (1966) used

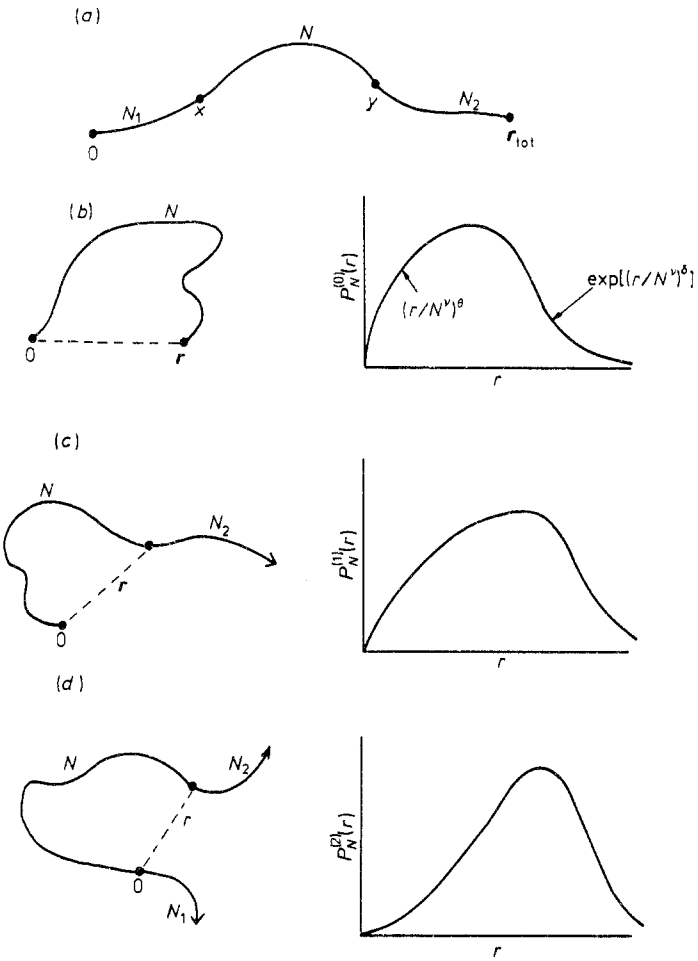

Figure 1. (*a*) The general chain configuration from which the probability distribution functions considered in this paper are derived. The usual endpoint problem is schematically defined in (*b*). The distribution function is sketched on the right to illustrate its physical features: it goes to 0 at the origin with infinite slope ($\theta < 1$), and it decays with a power of an exponential for large r. (*c*) The interior–endpoint problem. The arrow at the end of the chain indicates the limit $N_2 \to \infty$. Here, the decay of the distribution function is less steep near the origin than in (*a*), and the more sharply defined peak is located further to the right. (*d*) The interior–interior problem. When 0 and $\mathbf{r}$ are separated by a single lattice spacing, we obtain the interior contact probability. Here, the distribution function goes to zero near the origin with zero slope (for two dimensions only), and the central peak is much more pronounced.

analytic techniques to express δ in terms of ν, and found that $\delta = (1-\nu)^{-1}$. McKenzie and Moore (1971) employed a scaling approach to calculate both δ and θ in terms of other critical exponents for the polymer problem. McKenzie (1973) later used series techniques to study the detailed behaviour of equation (1).

The exponent θ gives a measure of the strength of the excluded volume interaction at small distances and is related to the initial ring closure probability, a quantity which has been studied in detail (Martin *et al* 1966, Sykes *et al* 1972 a,b and references

therein). From these studies it was found that $\theta = \frac{4}{9}$ for $d = 2$, and that $\theta = \frac{7}{36}$ for $d = 3$. More recently, des Cloizeaux (1974) also calculated δ and θ based on a Lagrangian field theory for the n-vector spin model in the limit $n \to 0$, a limit which corresponds to the polymer problem (de Gennes 1972). From this, θ was found to be $(\gamma - 1)/\nu$, where γ is the polymer analogue of the susceptibility exponent.

The spatial correlations between endpoints have been the primary focus of previous investigations. This reflects, perhaps, the fact that one naturally focuses on the two endpoints. Additionally, in the $n \to 0$ limit of the usual n-vector model, only the endpoints of the chain can be studied. Thus the nature of the spatial correlations between *arbitrary* points of the chain is still poorly understood. However such correlations are relevant in many experimental studies; for example, in determining the radius of gyration and the hydrodynamic radius of a polymer chain. Therefore it is important to investigate theoretically the nature of the distribution function between arbitrary points of a polymer chain. Recently Schäfer and Witten (1977) have used ϵ-expansion techniques to derive scaling laws for the general correlation functions. Also, Croxton (1979) has employed a new diagrammatic method to study the mean separation of two interior points within a polymer chain. Very recently, des Cloizeaux (1980) has also used the ϵ-expansion to calculate the exponents which govern the short-range behaviour of the distribution functions in three dimensions.

In this article, we use exact enumeration techniques to study quantitatively the probability distribution function between arbitrary points of a polymer chain in both two and three dimensions, and to elucidate the asymptotic behaviour at both small and large distances. Qualitatively, we find that the correlations between two interior points are more 'rigid-rod'-like than that between two endpoints. That is, two interior points are more likely to be separated by their mean distance than are endpoints. This effect reflects additional excluded volume constraints imposed on a monomer within the interior of the chain. The additional interaction manifests itself in the exponents which describe the asymptotic behaviour of the probability distribution functions. The focus of our study is to present evidence that these exponents are different from the exponents of the usual endpoint distribution function.

In the next section, we shall first present a formulation of the problem, due primarily to the work of des Cloizeaux (1980). In § 3, we examine the behaviour of the previously unstudied interior–interior distribution function for small distances. Then in § 4, we turn to the behaviour of the various distribution functions at large distances. Finally, we present a summary in § 5.

2. Distribution functions for SAW's

In studying the correlations between arbitrary points of a polymer chain, des Cloizeaux (1980) has found that these correlations can be simply divided into three classes: endpoint–endpoint, endpoint–interior point, and interior point–interior point. Accordingly, des Cloizeaux introduced new probability distribution functions which correspond to the three classes as follows. Consider a SAW which begins at the origin and goes to $\boldsymbol{x}$ in N_1 steps, to $\boldsymbol{y}$ in N steps, and finally to $\boldsymbol{r}_{\text{tot}}$ in N_2 steps. We shall use the probability $P(0, \boldsymbol{x}, \boldsymbol{y}, \boldsymbol{r}_{\text{tot}}; N_1, N, N_2)$ to describe this configuration of $n = N_1 + N + N_2$ steps as indicated in figure 1(a). The usual endpoint distribution function can then be defined as (see figure 1(b))

$$P_N^{(0)}(\boldsymbol{r}) = P(0, 0, \boldsymbol{r}, \boldsymbol{r}; 0, N, 0), \tag{2a}$$

where the superscript 0 refers to the endpoint problem. Similarly, the distribution function between an endpoint and an interior point can be defined as (see figure 1(*c*))

$$P_N^{(1)}(\boldsymbol{r}) = \lim_{N_2 \to \infty} P(0, 0, \boldsymbol{r}, \boldsymbol{r}_{\text{tot}}; 0, N, N_2), \tag{2b}$$

where the superscript 1 refers to the endpoint–interior point problem.

At small distance scales, (2*a*) describes the ring closure probability, while (2*b*) describes the *limited* ring closure or 'tadpole' probability. The latter is the probability that a SAW terminates by intersecting with another point of the walk which is not an endpoint. Wall *et al* (1954) were the first to consider this problem, and they estimated that the ring and tadpole probabilities were approximately equal. Subsequent, more accurate studies by Trueman and Whittington (1972), Guttmann and Sykes (1973) and Whittington *et al* (1975) found a slight difference between these two probabilities, indicating the possibility that the distribution functions (2*a*) and (2*b*) are in different universality classes.

Finally, we may define the distribution function between two interior points as (see figure 1(*d*))

$$P_N^{(2)}(\boldsymbol{r}) = \lim_{N_1 \to \infty} \lim_{N_2 \to \infty} P(0, \boldsymbol{x}, \boldsymbol{y}, \boldsymbol{r}_{\text{tot}}; N_1, N, N_2), \tag{2c}$$

where $\boldsymbol{r} = \boldsymbol{y} - \boldsymbol{x}$, and the superscript 2 refers to the interior–interior problem.

Des Cloizeaux used the ϵ-expansion to study the small-distance behaviour of these distribution functions, and found that they all have the same scaling form, $P_N^{(i)}(\boldsymbol{r}) \sim N^{-d\nu} f^{(i)}(r/N^{\nu})$, with $f^{(i)}(z) \sim z^{\theta_i}$ for $z \ll 1$, with the exponents θ_i being different. For $d = 3$, his calculation gives $\theta_0 = 0{\cdot}273 \pm 0{\cdot}004$, $\theta_1 = 0{\cdot}459 \pm 0{\cdot}003$ and $\theta_2 = 0{\cdot}71 \pm 0{\cdot}05$ (see table 1). That is, the relative importance of the excluded volume interaction near the origin depends on the type of problem being considered. The series for determining θ_0 and θ_1 have already been derived (Martin *et al* 1966, Sykes *et al* 1972 a,b, Guttmann and Sykes 1973), and in the next section we calculate the series for the short-distance limit of the interior–interior distribution function in order to determine θ_2.

3. Small-distance behaviour

To probe the distribution function between interior points at small distances ($r \ll N^{\nu}$), we require the analogue of the ring (or tadpole) closure probability. More correctly, we do not want the closure probability, but rather the probability for forming a nearest-neighbour contact. Because this quantity depends only on the scaling variable r/N^{ν}, finding the N-dependence of the probability for *fixed spatial separation of the contact* also gives its r-dependence. We therefore consider $P(0, \boldsymbol{x}, \boldsymbol{y}, \boldsymbol{r}_{\text{tot}}, N_1, N, N_2)$ for $|\boldsymbol{y} - \boldsymbol{x}| = l$, where l is a single lattice spacing. This gives the probability that two points separated by N bonds within an n-step SAW are nearest neighbours. We call this quantity the 'interior contact' probability $p_n(N)$, and this is the analogue of the contact probabilities in the ring and tadpole problems. In fact, all three contact probabilities are appropriate cases of the interior–interior distribution function at short distances. For example, if $N_1/N \to 0$ or $N_2/N \to 0$, a crossover to the probability of tadpole formation occurs. Moreover in the limit that both N_1 and $N_2 \to 0$, we recover simply the ring closure probability.

For our calculation, we choose $N_1 = N_2$ whenever possible. This choice minimises the crossover effects due to the tadpole problem. Sometimes we are obliged to choose

Table 1. Summary of current estimates for the short- and large-distance decay exponents for the three probability distribution functions considered in this work.

	$d=2$	$d=3$
θ_0	$\frac{4}{9}$[a,b]	$\frac{7}{36}$[a] $0{\cdot}275\pm0{\cdot}002$[b] $0{\cdot}273\pm0{\cdot}004$[c']
θ_1	$0{\cdot}84\pm0{\cdot}01$[d] $0{\cdot}84\pm0{\cdot}13$[e]	$0{\cdot}61\pm0{\cdot}17$[e] $0{\cdot}70\pm0{\cdot}12$[f] $0{\cdot}459\pm0{\cdot}003$[c]
θ_2	$2{\cdot}0$[c'] $1{\cdot}93\pm0{\cdot}27$[i]	$0{\cdot}71\pm0{\cdot}05$[c] $0{\cdot}67\pm0{\cdot}34$[i]
δ_0	$4{\cdot}0$[g,h]	$2{\cdot}5$[g,h]
δ_1	$4{\cdot}5\pm0{\cdot}4$[i]	$2{\cdot}6\pm0{\cdot}06$[i]
δ_2	$4{\cdot}6\pm0{\cdot}6$[i]	——

[a] Martin *et al* 1966
[b] des Cloizeaux 1974
[c] des Cloizeaux 1980—results of 2nd order ϵ-expansion
[c'] des Cloizeaux 1980—results of 1st order ϵ-expansion
[d] Trueman and Whittington 1972
[e] Guttmann and Sykes 1973
[f] Whittington *et al* 1975
[g] Domb *et al* 1965
[h] Fisher 1966
[i] This work

$N_1 = N_2 + 1$, when $n = N_1 + N + N_2$ is an odd number and N is even (or *vice versa*). This condition introduces some even–odd oscillations in our series, but this is not a serious problem. Additionally, we consider close-packed lattices only, where N can be both even or odd. On loose-packed lattices, N can be odd only (when l is a single lattice spacing), and even though we may enumerate longer walks, the corresponding data are not sufficiently well-behaved to give predictions as accurate as those on close-packed lattices.

Our data for the triangular and FCC lattices are given in table 2. Each row corresponds to a fixed number of total bonds, n, and each column corresponds to a fixed number of bonds, N, between the contact. The entries thus give the number of SAW's with an interior contact in the middle of the walk for fixed n and N. Other nearest-neighbour contacts may also occur, but they are not of relevance for the problem considered here. From the tables, we obtain the interior contact probability $p_n(N)$ by dividing each entry by the total number of SAW's of that order. We then extrapolate this probability to $n \to \infty$, while N remains fixed, in order to obtain the asymptotic contact probability $p(N)$ between two interior points within an infinitely long chain (last row of each table). We accomplish this by using Neville tables to perform linear, quadratic, cubic, etc extrapolations based on alternate pairs of data points. This type of extrapolation is called for because the series derived from considering both interior segments in the centre of a chain, and those offset by one bond from the centre, exhibit even–odd oscillations. For the first few N, there are sufficient terms in the series for $p_n(N)$ to give quite accurate asymptotic estimates. However the series are progres-

Table 2(*a*). Self-avoiding walk data on the triangular lattice. Each row corresponds to a given number of total bonds in the walk (beginning at $n = 1$). The Nth column gives the number of walks in which there are N bonds between an interior contact occurring in the 'middle' of the walk. Here 'middle' means that the contact occurs exactly in the centre of the walk if n and N are both even or both odd, while the contact is offset by one bond from the centre otherwise. The first column is the total number of all walks, and the upper right diagonal is the total number of ring closures of $n + 1$ steps. The lower portion of the table is the continuation of the table to the right. The closure probability $p_n(N)$ is found by dividing each entry by the total number of walks of that order. The bottom row then gives the extrapolated value of this closure probability, $p(N) = \lim_{n\to\infty} p_n(N)$.

n/N	1	2	3	4	5	6	7
1	6						
2	30	12					
3	138	48	24				
4	618	180	84	60			
5	2 730	792	264	192	180		
6	11 946	3 444	1 128	528	552	588	
7	51 882	15 000	4 728	2 196	1 416	1 728	1 968
8	224 130	64 932	20 304	8 928	5 616	4 236	5 676
9	964 134	280 200	86 496	37 776	21 576	16 152	13 692
10	4 133 166	1 204 572	369 732	158 160	90 480	59 004	49 968
11	17 668 938	5 159 448	1 573 608	670 632	374 928	245 688	172 908
12	75 355 206	22 043 292	6 703 068	2 828 724	1 580 256	1 009 500	712 380
13	320 734 686	93 952 428	28 474 704	11 977 356	6 620 904	4 233 528	2 891 640
14	1 362 791 250	399 711 348	120 922 272	50 553 456	27 902 556	17 637 600	12 073 308
	$p(N)$	= 0·298 2	0·088 2	0·034 5	0·018 4	0·011 5	0·007 7
		±6	±6	±7	±8	±10	±10

n/N	8	9	10	11	12	13	14
8	6 840						
9	19 512	24 240					
10	46 932	68 700	87 252				
11	164 988	165 840	246 840	318 360			
12	543 948	565 668	599 952	900 432	1 173 744		
13	2 212 308	1 795 920	1 998 456	2 204 508	3 323 376	4 366 740	
14	8 849 472	7 187 256	6 168 444	7 215 720	8 194 560	12 385 836	4 366 740
	0·005 0	0·003 5					
	±10	±18					

sively shorter for larger N and the uncertainties associated with extrapolation correspondingly increase. The error bars given in the last row of the tables represent subjective estimates of the uncertainties based on the Neville table analysis.

Next we need to find the dependence of the probability, $p(N)$, on N. According to equation (1), this probability should vary as $N^{-(d+\theta_2)\nu}$. Therefore we plot $p(N)$ versus N on a double logarithmic scale (see figure 2) and use a least-squares fit to determine the slope of the straight line which best fits the data points. We estimate the error associated with this slope by the following procedure. First we successively delete the first few data points, and calculate the slope (by least squares) of the straight line which best fits these subsets of data points. The variation of the slopes between subsets

Table 2(*b*). The same SAW data as in (*a*) for the FCC lattice.

n/N	1	2	3	4	5
1	12				
2	132	48			
3	1 404	480	264		
4	14 700	4 656	2 496	1 680	
5	152 532	47 760	22 800	15 624	11 640
6	1 573 716	485 904	229 368	133 440	102 936
7	16 172 148	4 972 032	2 287 896	1 321 008	874 272
8	165 697 044	50 692 272	23 218 344	12 955 296	8 541 048
9	1 693 773 924	517 215 774	234 741 432	130 570 128	82 600 248
10	17 281 929 564	5 265 877 872	2 384 687 064	1 310 778 864	827 100 192
	$p(N)$	$=0{\cdot}301\,0$	$0{\cdot}132\,5$	$0{\cdot}069\,8$	$0{\cdot}043\,0$
		± 10	± 10	± 20	± 20

n/N	6	7	8	9	10
6	86 352				
7	751 200	673 104			
8	6 269 136	5 789 472	5 424 768		
9	60 512 064	47 765 256	46 292 256	44 828 400	
10	577 866 000	426 253 080	379 082 784	380 448 408	377 814 528
	$0{\cdot}028\,0$	$0{\cdot}021\,0$			
	± 30	± 40			

indicates the presence and magnitude of possible systematic error. In addition, we also find the slopes for data in which selected points have been moved to the edge of an error bar. Combining these two sources of uncertainties gives confidence limits of the size of the error. Thus we estimate that $(d+\theta_2)\nu = +2{\cdot}16 \pm 0{\cdot}20$ on the FCC lattice, and $(d+\theta_2)\nu = +2{\cdot}95 \pm 0{\cdot}20$ on the triangular lattice. Using the estimate of $0{\cdot}588$ for ν in three dimensions (Le Guillou and Zinn-Justin 1977) leads to $\theta_2 = 0{\cdot}67 \pm 0{\cdot}34$ on the FCC lattice. On the triangular lattice, we use the Flory value of $0{\cdot}75$ for ν to yield $\theta_2 = 1{\cdot}93 \pm 0{\cdot}27$.

The three-dimensional result is in good agreement with the prediction of $\theta_2 = 0{\cdot}71$ from the second-order ϵ-expansion of des Cloizeaux (1980). In two dimensions the second-order expansion is poorly behaved, although the first-order term gives $\theta_2 = 2$ in close agreement with our estimate. It is also interesting that the N dependence of the interior contact probability is very different from the N dependence of the ring and tadpole probabilities in $d = 2$ (although for $d = 3$, the contact probabilities have nearly the same N dependence). This shows that excluded volume effects are very strong when two interior points are nearby, even more so than when an interior point and an endpoint are nearby.

4. Large-distance behaviour

To obtain a qualitative understanding of the properties at large distance scales ($r \gg N^{\nu}$), let us consider the case $N = 7$ for the three distribution functions on the square lattice

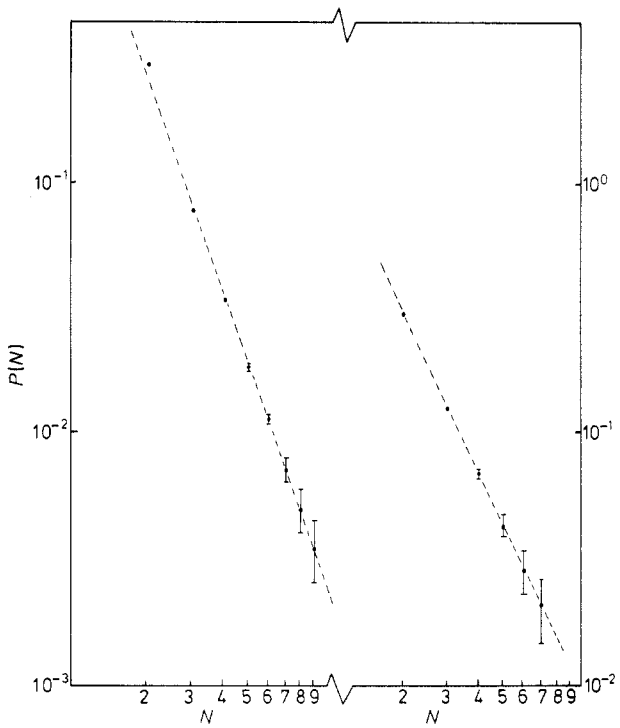

Figure 2. A plot of $\log p(N)$ versus $\log N$ in order to estimate the exponent $(d+\theta_2)\nu$. The left-hand portion shows data from the triangular lattice, and a linear least-squares fit (shown dashed) yields the estimate $(d+\theta_2)\nu = +2{\cdot}95 \pm 0{\cdot}20$. The right-hand portion shows data from the FCC lattice. Here the least-squares fit yields the estimate $(d+\theta_2)\nu = +2{\cdot}16 \pm 0{\cdot}20$.

(see figure 3). To define $P_7^{(1)}(\boldsymbol{r})$, we consider all 14-step SAW's, and ask for the probability distribution between one end and the midpoint. The midpoint is the most natural choice for defining $P_N^{(1)}(\boldsymbol{r})$, although in the $N \to \infty$ limit, any interior point could equally well be chosen as long as N_1/N does not approach zero. However, for the relatively short chains considered here, choosing the interior point close to the end of the chain gives behaviour indicative of the endpoint problem. Therefore to minimise such crossover effects, we have defined $P_N^{(1)}(\boldsymbol{r})$ using an endpoint and the midpoint.

Similarly, to define $P_7^{(2)}(\boldsymbol{r})$, we consider all 21-step SAW's, and examine the probability distribution between two points which trisect the chain. Again there is considerable freedom in choosing the two interior points, and our choice minimises the various crossover effects mentioned previously.

In addition to $P_N^{(i)}(\boldsymbol{r})$, we have also considered $\tilde{P}_N^{(i)}(x)$, the distribution function for the probability that the absolute value of one cartesian coordinate of $\boldsymbol{r}$ equals x. One advantage of this distribution function is that it is smoother than $P_N^{(i)}(\boldsymbol{r})$, and is therefore more suited to visual inspection (see figure 4). The use of $\tilde{P}^{(i)}$ presumes that the radial distribution function is spherically symmetric, so that the projection of this function onto one coordinate axis will give unbiased results. The spherical symmetry of $\tilde{P}^{(0)}$ has been previously established by Domb *et al* (1965), and *a priori*, there is no reason to doubt that $\tilde{P}^{(1)}$ and $\tilde{P}^{(2)}$ are not also spherically symmetric since there is no preferred spatial direction. Consequently we have assumed this result for the distribution functions in the analysis that follows.

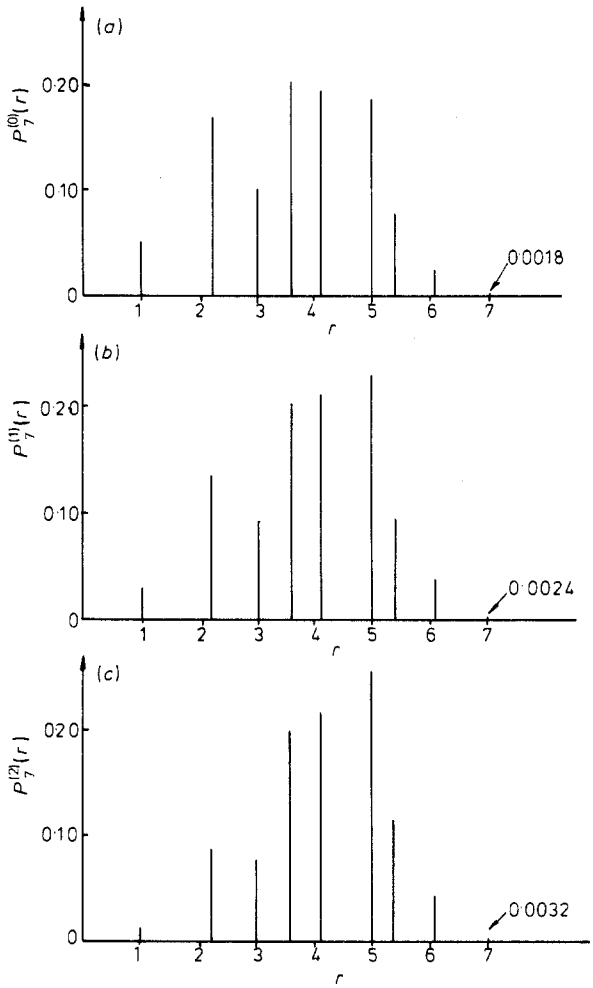

Figure 3. The radial probability distribution functions on the square lattice for the three problems defined in figure 1: (*a*) endpoint–endpoint, (*b*) endpoint–interior, (*c*) interior–interior. Data are from the square lattice, and there are seven bonds between the origin and *r*. Notice that the data exhibit the qualitative features outlined in figure 1.

For the endpoint problem, the earlier study of Domb *et al* was based on fitting $\tilde{P}^{(0)}$ to

$$A \exp[-(x/N^{\nu})^{\delta_0}], \tag{3a}$$

to find the exponent δ_0 describing the decay of the distribution function at large distances. On the square lattice, there is a slight dip at the origin in $\tilde{P}^{(0)}$ which is not accounted for by the exponential (see figure 4). This was not judged to be serious for the endpoint problem, but for the other two problems, the dip near the origin is much more prominent. As a result, a simple exponential is not adequate to describe the data for all *r*. We have therefore analysed the *radial* distribution functions, in order properly to account for the anomalous small-distance behaviour. Thus instead of using (3*a*), we have attempted to fit our data to the function

$$P_N^{(i)}(r) \sim A(r/N^{\nu})^{\theta_i} \exp[-(r/N^{\nu})^{\delta_i}], \tag{3b}$$

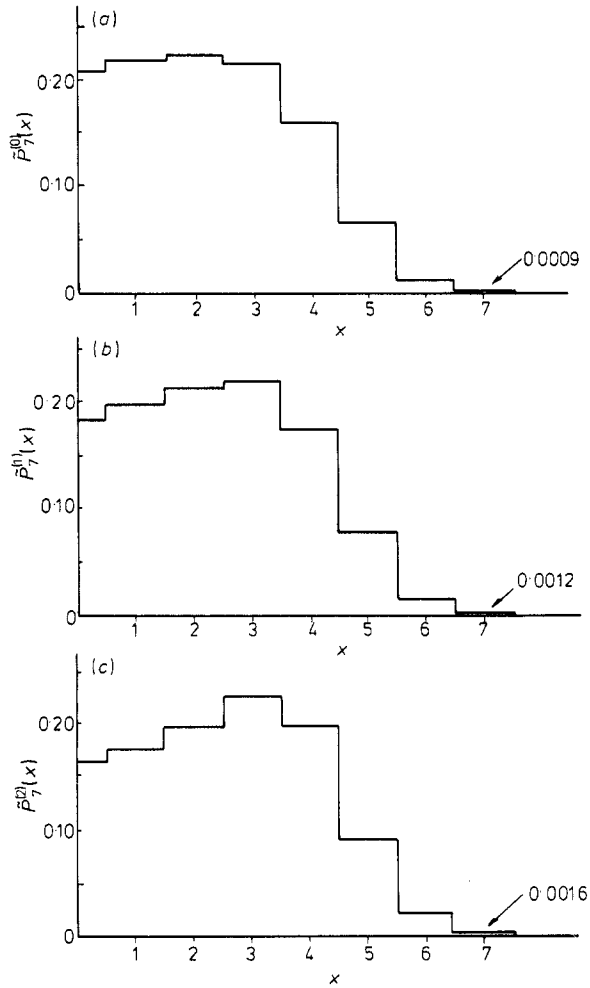

Figure 4. The projection of the data of figure 3 onto one cartesian coordinate. This defines the cartesian probability distribution function $\tilde{P}_N^{(i)}(x)$ for the three problems (a), (b) and (c). For these cases, the relative magnitudes of the dips at the origin (ratio of peak height to height at the origin) are 6·7%, 12·4% and 27·5% respectively.

where δ_i now describes the decay of $P_N^{(i)}(\boldsymbol{r})$ at large distances. While each factor is valid only in one regime (either $r \ll N^\nu$, or $r \gg N^\nu$), the product fits the data quite well for all $\boldsymbol{r}$. Furthermore, in the region where one factor is rapidly varying; the other is virtually constant. Thus for $r \ll N^\nu$, $\exp[-(r/N^\nu)^{\delta_i}] \approx 1$, while for $r \gg N^\nu$, the decay is purely exponential with only a power law prefactor. Consequently, the effects introduced by the influence of the slowly varying factor on the more rapidly varying one should be small.

In order to calculate the exponents δ_1 and δ_2, we have considered all SAW's of up to 21 bonds on the square lattice, and up to 14 bonds on the simple cubic lattice. Close-packed lattices were not considered here because it was not possible to obtain series of sufficient length to extrapolate with any confidence. From our enumeration on the square lattice, we have calculated $P^{(0)}$ for $N = 1, 2, \ldots, 20$, $P^{(1)}$ and $\tilde{P}^{(1)}$ for

Table 3. Self-avoiding walk data on the square lattice. Walks are classified according to the absolute value of the vector joining an endpoint with the midpoint of the walk. Only the values for $|x| \geq |y|$ are shown.

No. of bonds	x	y	$n(x, y)$	x	y	$n(x, y)$	x	y	$n(x, y)$
2	1	0	6						
4	1	1	56						
	2	0	22						
6	1	0	64						
	2	1	276						
	3	0	50						
8	1	1	800	3	1	1 032			
	2	0	636	4	0	138			
	2	2	1 504						
10	1	0	1 196	3	2	6 896			
	2	1	6 248	4	1	3 572			
	3	0	3 760	5	0	378			
12	1	1	20 408	3	1	42 372	4	2	28 340
	2	0	13 612	3	3	37 280	5	1	11 752
	2	2	37 472	4	0	17 780	6	0	1 030
14	1	0	35 636	4	1	239 208	5	2	108 630
	2	1	163 796	4	3	177 148	6	1	37 376
	3	0	109 060	5	0	74 220	7	0	2 790
	3	2	239 628						
16	1	1	634 480	4	0	728 772	6	0	285 620
	2	0	404 792	4	2	1 433 436	6	2	392 640
	2	2	1 128 560	4	4	953 024	7	1	115 872
	3	1	1 238 448	5	1	1 177 336	8	0	7 534
	3	3	1 423 632						
18	1	0	1 163 784	4	3	8 429 892	6	3	3 121 496
	2	1	5 264 464	5	0	4 222 060	7	0	1 039 528
	3	0	3 343 328	5	2	7 765 980	7	2	1 368 136
	3	2	7 816 800	5	4	4 625 852	8	1	352 528
	4	1	8 543 988	6	1	5 251 236	9	0	20 294
20	1	1	21 679 264	4	4	49 301 144	7	1	21 768 160
	2	0	13 609 956	5	1	53 344 972	7	3	12 045 504
	2	2	37 720 192	5	3	47 499 624	8	0	3 628 184
	3	1	41 073 680	5	5	24 804 832	8	2	4 619 284
	3	3	50 985 272	6	0	21 871 168	9	1	1 056 008
	4	0	24 584 804	6	2	34 817 560	10	0	54 546
	4	2	52 254 172	6	4	20 775 608			

$N = 1, 2, \ldots, 10$, and $P^{(2)}$ and $\tilde{P}^{(2)}$ for $N = 1, 2, \ldots, 7$ (see tables 3 and 4). On the simple cubic lattice, we have calculated $\tilde{P}^{(1)}$ for $N = 1, 2, \ldots, 7$ (see table 5). We did not consider $\tilde{P}^{(2)}$ because our data extends only to $N = 5$, and this was insufficient to probe asymptotic behaviour.

One way to fit our data with the trial distribution functions defined by (3*b*) is to calculate the reduced radial moments

$$m_{2k}^{(N)} = \langle r_N^{2k} \rangle / (\langle r_N^2 \rangle)^k \tag{4}$$

Table 4. Classification of SAW's on the square lattice according to the absolute value of the vector joining two points which trisect the chain.

No. of bonds	x	y	$n(x, y)$	x	y	$n(x, y)$	x	y	$n(x, y)$
3	1	0	18						
6	1	1	464						
	2	0	158						
9	1	0	860						
	2	1	6 036						
	3	0	1 238						
12	1	1	28 240	3	1	64 264			
	2	0	29 732	4	0	9 434			
	2	2	89 832						
15	1	0	76 624	3	2	1 149 776			
	2	1	740 000	4	1	624 356			
	3	0	546 504	5	0	71 038			
18	1	1	3 699 168	3	1	15 555 800	4	2	13 045 588
	2	0	3 488 760	3	3	16 862 560	5	1	5 662 832
	2	2	12 489 312	4	0	7 523 056	6	0	527 810
21	1	0	12 272 468	4	1	257 972 860	5	2	137 267 196
	2	1	107 273 676	4	3	219 053 104	6	1	49 355 976
	3	0	93 755 008	5	0	88 916 956	7	0	3 879 186
	3	2	234 656 584						

for the three distribution functions and extrapolate to $N \to \infty$ as indicated by the last row in tables 6 and 7. Here $\langle r_N^{2k} \rangle$ is the mean value of r^{2k} between the two points under study, and N indicates that the origin and r are separated by N bonds. The series for $m_{2k}^{(N)}$ again exhibit even–odd oscillations and we therefore use Neville tables based on extrapolating alternate pairs of points to estimate the asymptotic behaviour of $m_{2k} = \lim_{N\to\infty} m_{2k}^{(N)}$. We then compare the results of this extrapolation with the moments derived from (3*b*) for various values of δ_i. In two dimensions, the reduced moments of the function (3*b*) can be expressed in terms of gamma functions as

$$m_{2k} = \Gamma[(2k + \theta_i + 2)/\delta_i]/\Gamma[(\theta_i + 2)/\delta_i]. \tag{5}$$

We then vary the trial value of δ_i until the best fit between the two sets of moments is found.

To test whether the procedure described above is valid, we first consider the endpoint distribution function on the square lattice. We use the well-established value $\theta_0 = \frac{4}{9}$, which follows from the ring closure probability varying as $N^{-11/6}$ (Martin *et al* 1966, Sykes *et al* 1972 a,b), and calculate m_{2k} from equation (5) for a range of values of δ_0. Choosing $\delta_0 = 4$ gives

$$m_4 = 1{\cdot}46, \qquad m_6 = 2{\cdot}65, \qquad m_8 = 5{\cdot}61, \qquad m_{10} = 13{\cdot}35, \qquad m_{12} = 34{\cdot}9,$$

and these numbers give the best fit to the extrapolated moments in table 6(*a*). Thus, to calculate δ_0, one can consider the radial distribution function as well as the cartesian distribution function. This is an extremely useful check for the ensuing analysis.

For the endpoint–interior problem on the square lattice, we use $\theta_1 = 0{\cdot}84$ in equation (5)—a result which follows from the tadpole probability varying as $N^{-2{\cdot}13}$

Table 5. Classification of SAW's on the simple cubic lattice according to the absolute value of the vector joining an endpoint with the midpoint of the walk.

No. of bonds	x	y	z	$n(x, y, z)$	x	y	z	$n(x, y, z)$
2	1	0	0	30				
4	1	1	0	192				
	2	0	0	50				
6	1	0	0	752				
	1	1	1	5 472				
	2	1	0	1 412				
	3	0	0	242				
8	1	1	0	31 136	2	2	0	13 536
	2	0	0	12 280	3	1	0	9 112
	2	1	1	52 976	4	0	0	1 170
10	1	0	0	167 384	3	1	1	426 288
	1	1	1	1 010 256	3	2	0	108 096
	2	1	0	459 520	4	1	0	54 724
	2	2	1	632 992	5	0	0	5 602
	3	0	0	122 928				
12	1	1	0	7 419 160	3	3	0	1 028 928
	2	0	0	3 942 488	4	0	0	998 952
	2	1	1	15 453 744	4	1	1	3 070 224
	2	2	0	6 831 632	4	2	0	775 248
	2	2	2	9 009 840	5	1	0	314 328
	3	1	0	5 103 436	6	0	0	26 746
	3	2	1	6 059 808				
14	1	0	0	43 866 024	3	3	1	67 268 448
	1	1	1	277 243 200	4	1	0	47 222 024
	2	1	0	139 655 140	4	1	1	20 563 216
	2	2	1	239 133 360	4	3	0	8 570 852
	3	0	0	56 119 944	5	0	0	7 223 976
	3	1	1	193 477 792	5	2	0	5 178 888
	3	2	0	81 551 468	6	1	0	1 749 680
	3	2	2	100 187 296	7	0	0	127 338

(Trueman and Whittington 1972). With the value $\delta_1 = 4{\cdot}5$ this yields for the reduced moments

$$m_4 = 1{\cdot}36, \qquad m_6 = 2{\cdot}24, \qquad m_8 = 4{\cdot}20, \qquad m_{10} = 8{\cdot}71, \qquad m_{12} = 19{\cdot}7,$$

and these numbers give the best fit to the extrapolation in table 6(b). Finally, for the interior–interior problem, we use $\theta_2 = 1{\cdot}93$ found in the previous section for the triangular lattice, and we assume that this exponent is universal for all two-dimensional lattices. The choice $\delta_2 = 4{\cdot}6$ yields

$$m_4 = 1{\cdot}25, \qquad m_6 = 1{\cdot}81, \qquad m_8 = 2{\cdot}96, \qquad m_{10} = 5{\cdot}27, \qquad m_{12} = 10{\cdot}1.$$

These moments are best fits to the extrapolation in table 6(c). Thus we conclude that $\delta_0 = 4{\cdot}0$ in agreement with the currently accepted result, and that $\delta_1 = 4{\cdot}5$, and $\delta_2 = 4{\cdot}6$.

We determine a lower bound to the estimates for δ_1 and δ_2 as follows. We take the values for θ_i to be those at the upper limit of the quoted error bars; that is we take

Table 6. (*a*) The reduced radial moments m_{2k} of the distribution function $P_N^{(0)}(r)$ on the square lattice, defined by equation (4). The last line gives the extrapolation of each column. (*b*) The reduced radial moments of the distribution function $P_N^{(1)}(r)$ on the square lattice. (*c*) The reduced radial moments of the distribution function $P_N^{(2)}(r)$ on the square lattice.

(*a*) *n*			*m*		
4	1·252 583	1·786 574	2·796 211	4·745 248	8·665 928
5	1·297 136	1·935 567	3·181 652	5·663 703	10·839 803
6	1·301 491	1·965 000	3·281 461	5·934 912	11·517 606
7	1·329 399	2·062 932	3·553 904	6·637 389	13·284 960
8	1·331 255	2·079 602	3·618 281	6·834 285	13·828 458
9	1·349 514	2·146 053	3·811 913	7·361 467	15·230 960
10	1·351 057	2·158 885	3·862 835	7·525 707	15·715 202
11	1·363 710	2·206 251	4·005 540	7·929 540	16·835 737
12	1·365 010	2·216 506	4·046 860	8·067 245	17·259 662
13	1·374 280	2·251 967	4·156 392	8·386 175	18·173 079
14	1·375*S*4343	2·260 226	4·190 186	8·501 634	18·539 867
15	1·382 474	2·287 943	4·277 417	8·761 166	19·301 388
16	1·383 328	2·294 636	4·305 271	8·858 349	19·617 843
17	1·388 998	2·316 952	4·376 546	9·074 048	20·263 000
18	1·389 694	2·322 474	4·399 865	9·156 802	20·537 816
19	1·394 314	2·340 844	4·459 246	9·339 019	21·091 411
20	1·394 890	2·345 471	4·479 039	9·410 265	21·331 832
	1·46 ± 0·01	2·64 ± 0·05	5·60 ± 0·10	13·0 ± 0·5	34 ± 2
(*b*)					
2	1·000 000	1·000 000	1·000 000	1·000 000	1·000 000
4	1·118 827	1·366 384	1·767 517	2·364 442	3·221 139
6	1·180 592	1·523 992	2·140 170	3·275 234	5·416 776
8	1·225 174	1·690 656	2·549 973	4·163 489	7·304 960
10	1·249 121	1·772 191	2·754 872	4·627 016	8·345 361
12	1·263 946	1·828 918	2·908 831	4·995 488	9·191 805
14	1·276 968	1·876 532	3·040 178	5·320 216	9·958 755
16	1·286 270	1·913 140	3·145 912	5·592 960	10·627 680
18	1·294 448	1·944 546	3·237 469	5·834 232	11·234 993
20	1·300 866	1·970 313	3·314 714	6·043 395	11·776 308
	1·36 ± 0·02	2·25 ± 0·05	4·15 ± 0·20	8·5 ± 0·7	19 ± 2
(*c*)					
3	1·000 000	1·000 000	1·000 000	1·000 000	1·000 000
6	1·122 063	1·382 672	1·815 435	2·475 410	3·446 103
9	1·152 168	1·461 421	2·022 089	3·014 451	4·754 586
12	1·177 332	1·536 555	2·180 665	3·343 033	5·495 648
15	1·191 058	1·582 974	2·287 906	3·561 531	5·943 359
18	1·201 776	1·620 940	2·381 761	3·763 094	6·357 080
21	1·209 008	1·647 671	2·451 321	3·919 540	6·686 247
	1·28 ± 0·03	1·85 ± 0·07	3·0 ± 0·2	5·25 ± 0·7	10 ± 2

$\theta_1 = 0{\cdot}84 + 0{\cdot}015 = 0{\cdot}86$ (Trueman and Whittington 1972) and $\theta_2 = 1{\cdot}95 + 0{\cdot}27 = 2{\cdot}23$ (our result). Since the reduced moments m_{2k} calculated from equation (5) decrease when either θ_i or δ_i is increased, we must now use a lower δ_i in order to fit with the extrapolated m_{2k} given in tables 6(*b*) and 6(*c*). The lowest value of δ_i which gives a calculated m_{2k} just consistent with the upper limit of the error bars for the extrapolated

Table 7. The reduced cartesian moments of the distribution function $\tilde{P}_N^{(1)}(x)$ on the simple cubic lattice.

n	m				
4	2·523 864	9·491 798	43·361 361	210·687 907	1040·822 469
6	2·463 659	9·182 760	43·714 270	243·446 481	1491·905 589
8	2·446 661	9·033 837	43·205 664	247·297 689	1608·882 245
10	2·451 683	9·025 526	43·183 891	249·433 290	1659·756 523
12	2·456 470	9·039 031	43·241 738	250·568 703	1682·958 140
14.	2·465 084	9·085 434	43·510 215	252·710 255	1706·359 332
	2·58 ± 0·02	10·14 ± 0·3	53 ± 0·3	310 ± 15	2400 ± 150

m_{2k} yields our lower bound for δ_i. This takes into account both the uncertainties in estimating θ_i and extrapolating the reduced moment sequences.

Because the value of θ_1 is fairly accurately determined, we therefore estimate that $\delta_1 = 4{\cdot}5 \pm 0{\cdot}4$. For δ_2, the shorter reduced moment series and the larger error bars for θ_2 combine to yield the estimate $\delta_2 = 4{\cdot}6 \pm 0{\cdot}6$. In summary, our analysis indicates that both δ_1 and δ_2 are greater than δ_0. The higher values of δ_1 and δ_2 over δ_0 are consistent with the interpretation that the effect of the remainder of the chain is to provide a net inward force on the segment between 0 and $\boldsymbol{r}$ *at large distance scales only.*

For $d > 2$, it is easier for the remainder of the chain to penetrate into the region occupied by the segment between 0 and $\boldsymbol{r}$, and hence the relative magnitude of the inward force is decreased. Hence the difference between δ_0, δ_1 and δ_2 should be reduced, and on the simple cubic lattice we present evidence that this appears to be the case. Additionally, on this lattice the problems associated with the analysis of the radial distribution function can be avoided. Here, the cartesian distribution function does not have a dip near the origin, owing to weaker excluded volume effects (see figure 5). Consequently, we have analysed the cartesian function, and now fit the decay of the distribution to the simple exponential $\tilde{P}_N^{(1)}(x) \sim A \exp[-(x/N^{\nu})^{\delta_1}]$. Thus our analysis for δ_1 is no longer influenced by possible errors in θ_1. Choosing $\delta_1 = 2{\cdot}6$ in (6) gives for the reduced moments

$$m_4 = 2{\cdot}58, \qquad m_6 = 10{\cdot}1, \qquad m_8 = 52{\cdot}1, \qquad m_{10} = 327, \qquad m_{12} = 2408,$$

and these are a good fit for the extrapolated values quoted in table 7. Here our only source of error stems from extrapolating the series for m_{2k}. Although the series are relatively short, we are reasonably confident that our estimate for δ_1 is accurate to within 0·06.

5. Summary

We have studied the probability distribution functions between two endpoints, an endpoint and an interior point, and two interior points for self-avoiding walks in both two and three dimensions. For small distance scales we consider the correlations between interior points, and define an appropriate 'interior contact' probability. From the form of the scaling function f defined by equation (1) this probability should vary with N as $N^{-(d+\theta_2)\nu}$. We estimate from our data that $(d+\theta_2)\nu = +2{\cdot}16 \pm 0{\cdot}20$ on the FCC lattice, leading to $\theta_2 = 0{\cdot}67 \pm 0{\cdot}34$ for the exponent describing the decay of the

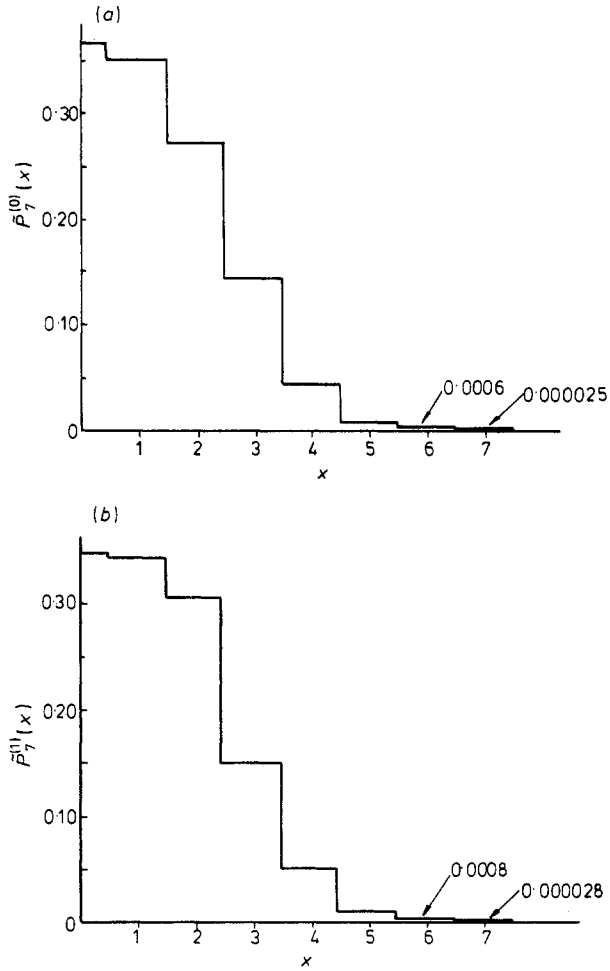

Figure 5. The cartesian probability distribution function for SAW's on the simple cubic lattice. Part (*a*) shows the endpoint problem for 7-step walks, and part (*b*) shows the endpoint–interior problem for 14-step walks.

distribution function at small distances. On the triangular lattice, we estimate that $(d+\theta_2)\nu = +2{\cdot}95 \pm 0{\cdot}20$, corresponding to $\theta_2 = 1{\cdot}93 \pm 0{\cdot}27$. These values indicate that the probability of a nearest-neighbour contact between two monomers within the interior of a chain is much less likely to occur than between two endpoints separated by the same number of monomers.

For large r, we find that the tails of the distribution functions vary as $\exp[-(r/N^{\nu})^{\delta_i}]$. On the square lattice, we estimate that $\delta_1 = 4{\cdot}5 \pm 0{\cdot}4$, and $\delta_2 = 4{\cdot}6 \pm 0{\cdot}6$ (compared with $\delta_0 = 4{\cdot}0$ for the endpoint distribution function). On the simple cubic lattice, we estimate δ_1 to be $2{\cdot}6 \pm 0{\cdot}06$ (compared with $\delta_0 = 2{\cdot}5$). The possible higher values for δ_1 and δ_2 over δ_0 indicate that it is less probable for an N-step segment in the interior of a longer chain to be in a stretched configuration than it is for a complete chain of N monomers. Coupled with the information at small distances, it appears that the correlations between monomers in the interior of a polymer chain are more rigid-rod-like in character than the correlations between end monomers.

Acknowledgments

I am grateful to M Daoud and T Witten for many stimulating discussions concerning this work. I wish to thank H Nakanishi and P J Reynolds for a critical reading of the manuscript, and valuable suggestions. I am especially indebted to the Boston University Computing Center for generously providing the necessary computer time, and related facilities for the completion of this project. I also thank the referees for helpful and constructive criticism. This work has been supported in part by the ARO, AFOSR, and by a grant from the Boston University Graduate School of Science.

References

des Cloizeaux J 1974 *Phys. Rev.* A **10** 1665–9
—— 1980 *J. Physique* **41** 223–28
Croxton C A 1979 *J. Phys. A: Math. Gen.* **12** 2487–95
Domb C, Gillis J and Wilmers G 1965 *Proc. Phys. Soc.* **85** 625–45
Fisher M E 1958 *Disc. Faraday Soc.* **25** 200
—— 1966 *J. Chem. Phys.* **44** 616–22
Fisher M E and Hiley B J 1961 *J. Chem. Phys.* **34** 1253–67
de Gennes P G 1972 *Phys. Lett.* **38**A 339–40
—— 1979 *Scaling Concepts in Polymer Physics* (Ithaca, NY: Cornell University Press)
Guttmann A J and Sykes M F 1973 *J. Phys. C: Solid St. Phys.* **6** 945–54
Le Guillou J C and Zinn-Justin J 1977 *Phys. Rev. Lett.* **39** 95–8
Martin J L, Sykes M F and Hioe F T 1966 *J. Chem. Phys.* **46** 3478–81
McKenzie D S 1973 *J. Phys. A: Math., Nucl. Gen.* **8** 338–52
McKenzie D S and Moore M A 1971 *J. Phys. A: Gen. Phys.* **4** L82–6
Schäfer L and Witten T A Jr 1977 *J. Chem. Phys.* **66** 2121–30
Sykes M F, Guttmann A J, Watts M G and Roberts P D 1972a *J. Phys. A: Gen. Phys.* **5** 653–60
Sykes M F, McKenzie D S, Watts M G and Martin J L 1972b *J. Phys. A: Gen. Phys.* **5** 661–6
Trueman R E and Whittington S G 1972 *J. Phys. A: Gen. Phys.* **5** 1664–8
Wall F T and Erpenbeck J J 1959 *J. Chem. Phys.* **30** 634–40
Wall F T, Hiller L A Jr and Wheeler D J 1954 *J. Chem. Phys.* **22** 1036–41
Whittington S G, Trueman R E and Wilker J B 1975 *J. Phys. A: Math. Gen.* **8** 56–60